Synthesis of Grafted Block Copolymers Based on ε-Caprolactone: Influence of Branches on Their Thermal Behavior

Mario D. Ninago,* Augusto G. O. De Freitas, Vivina Hanazumi, Paulo I. R. Muraro, Vanessa Schmidt, Cristiano Giacomelli, Andrés E. Ciolino, Marcelo A. Villar

Branched copolymers are a special class of polymeric materials in which are reflected the combined effects of polymer segments and architectural constraints of the branched architecture. This study employed two methodologies to obtain copolymers with different branching density. In the first case, poly(hydroxyethyl methacrylate-*graft*-poly(ε-caprolactone)-*block*-poly(ε-caprolactone), P(HEMA-*g*-PCL)-*b*-PCL, copolymers were synthesized by a "grafting through" method in a three-step reaction pathway involving ring opening polymerization (ROP) and radical addition fragmentation transfer (RAFT) polymerization. In the second case, a combination of simultaneous "grafting through" and "grafting from" methods in a one-pot RAFT and ROP reaction afforded P(HEMA-*co*-HEMA-*g*-PCL)-*b*-PCL comb-like copolymers with comparatively less dense branching. Samples with molar masses between 5500 and 46 000 g mol^{-1} and polydispersity indexes (M_w/M_n) lower than 1.3 were successfully obtained through both approaches. According to thermal analyses, the presence of branches reduces PCL melting temperature by as much as 20 °C, without affecting thermal stability. This fact was particularly evident for the most densely branched copolymers with higher molar masses. Nonisothermal crystallization process was successfully described using Ozawa's method, which showed a clear dependence of crystallization rate and cooling on grafting density.

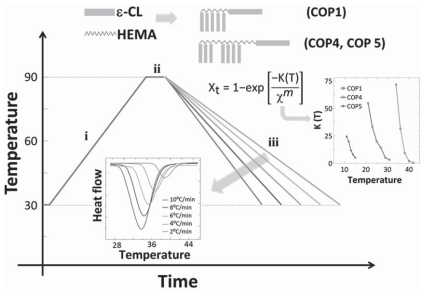

Dr. M. D. Ninago, V. Hanazumi, Dr. A. E. Ciolino, Dr. M. A. Villar
Planta Piloto de Ingeniería Química
PLAPIQUI (UNS-CONICET)
Departamento de IngenieríaQuímica
UNS, Camino "La Carrindanga" Km 7
8000 Bahía Blanca, Argentina
E-mail: mninago@plapiqui.edu.ar
A. G. O. De Freitas, P. I. R. Muraro, Dr. V. Schmidt, Dr. C. Giacomelli
Departamento de Química
Universidade Federal de Santa María
97105–900 Santa Maria-RS, Brazil

1. Introduction

Unlike linear diblock and triblock copolymers, branched polymers constitute a special kind of macromolecular architectures in which each molecule has more than two chain ends.[1] This particularity imparts unique physical and chemical properties that definitely influence their dynamics, bulk morphologies, and long-range nanoscale order.[2,3] Among the plethora of macromolecular structures that can be classified as ramified polymers, comb-like copolymers belong to a special class of branched macromolecules in which their "teeth" are distributed in

DOI: 10.1002/macp.201500248

a specific segment of the macromolecule. In its simplest structure, comb-like copolymers are a special class of polymeric materials in which "the handle of the comb" and the "backbone" are of one monomeric specie and the "teeth" are of another species, but many other alternatives are also possible.[4–6]

Branched macromolecular architectures are important from a scientific perspective because they exhibit properties that reflect the combined effects of thermodynamic incompatibility of the polymer segments and the architectural constraints of the branched architecture.[7,8] As in the case of dendrimers, branched copolymers exhibit physicochemical properties different from those of linear polymers of the same molar mass, such as multiend polymer chains,[9] lack of significant entanglement in the solid state,[10] high solubility in various solvents, and low melt viscosity.[11] The comprehensive understanding of the physicochemical behavior of this kind of copolymers is relevant if we take into account the fact that commercially synthesized copolymers frequently display some degree of branching. As it is well-known, many industrial polymer processing techniques (such as extrusion, molding, and melt spinning of synthetic fibers) involve polymer melts, and the presence of branches must be considered in order to effectively predict their behavior.

Moreover, nonisothermal crystallization analysis has attracted considerable attention in the field of polymer and engineering science in order to better understand industrial conditions for polymer processing. Nevertheless, scientific literature provides only few studies on the nonisothermal crystallization behavior of complex macromolecules (such as block copolymers) as well as the effect of macromolecular architecture on the crystallization kinetics. Due to those practical processes usually proceeded under nonisothermal crystallization conditions, it is of interest to study nonisothermal crystallization kinetics for understanding the actual behavior of polymer crystallization processes.[3,12–14]

PCL is an aliphatic and hydrophobic semicrystalline polyester derived from a ring opening polymerization (ROP) of the ε-caprolactone (ε-CL) monomer and has a relatively low melting point (60 °C). Furthermore, its biodegradability and ability to form compatible blends with a wide range of other polymers explain the broad field of applications.[15–17] Its physical properties and commercial availability makes it a good substitute for conventional nonbiodegradable polymers used not only for common applications but also as specialty polymers in medicine and agriculture.[16,18–24] On the other hand, poly(2-hydroxyethylmethacrylate) (PHEMA) is a useful material that finds commercial applications in soft contact lenses, as drug delivery scaffolds, and in biomedical engineering, among others.[22–25] In particular, PHEMA hydrogels with various degrees of crosslinking and hydrophilicity have found different biomedical applications.[22,25–28]

In this study, two methodologies were used to obtain well-defined block copolymers based on ε-CL with different branching density. In the first one, poly(hydroxyethylmethacrylate-*graft*-poly(ε-caprolactone)-*block*-poly(ε-caprolactone), P(HEMA-*g*-PCL)-*b*-PCL copolymers were synthesized by a "grafting through" method in a three-step reaction pathway involving ROP and radical addition fragmentation transfer (RAFT) polymerization. In the second one, a combination of simultaneous "grafting through" and "grafting from" methods in a one-pot RAFT and ROP reaction afforded P(HEMA-*co*-HEMA-*g*-PCL)-*b*-PCL. Obtained copolymers were chemically characterized by ^{1}H-nuclear magnetic resonance (^{1}H-NMR), size exclusion chromatography (SEC), Fourier transform infrared spectroscopy (FTIR). Their thermal transition and thermal stability were followed by differential scanning calorimetry (DSC) and thermogravimetric analysis (TGA). Moreover, nonisothermal crystallization process was performed by DSC, and the crystallization behavior was evaluated by using Ozawa's method in order to obtain kinetic parameters of interest. The half-life time of crystallization ($t_{1/2}$) and the *m* exponent, which are dependent on the nucleation and growth mechanism, were determined. Results obtained by these analyses were compared with the respective linear PCL homopolymer in order to explain the influence of branches on thermal and crystallization processes.

2. Experimental Section

2.1. Materials and Methods

2-Hydroxyethylmethacrylate (HEMA, Aldrich, 97%), ε-CL (Aldrich, 99%), diphenyl phosphate (DPP, 99%), 1,1′-azobis(cyclohexanecarbonitrile) (VAZO catalyst 88, Aldrich, 98%), toluene (Aldrich), methanol (Química Industrial), dimethylformamide (DMF, 99.8%), chloroform (Aldrich, 99.5%), deuterated chloroform ($CDCl_3$), and petroleum ether were used as solvents without any further purification. (Benzylsulfanylthiocarbonylsulfanyl) ethanol (BSTSE) chain transfer agent was prepared following a one-pot procedure previously described elsewhere.[3,29–31] The resulting BSTSE was further purified by column chromatography on silica using petroleum ether as eluent and recrystallized under cold conditions. On the other hand, a *model* PCL homopolymer was synthesized as reference material by employing classical anionic polymerization as described elsewhere (DP ≈ 100).[32–34]

2.1.1. Synthesis of P(HEMA-*g*-PCL)-*b*-PCL by "Grafting Through" (or Macromonomer) Method

Copolymers were prepared by a "grafting through" method consisting in the polymerization of PCL macromonomer (mPCL) mediated by a PCL macro chain transfer agent (PCL macroCTA). ROP of ε-CL initiated by HEMA afforded mPCL, whereas the reaction

initiated by BSTSE led to a PCL macroCTA. The same experimental conditions were applied in both ROP reactions, as follows: toluene (2.5 mL), ε-CL (2.06 g, 17.52 mmol), initiator (BSTSE 0.285 g, or HEMA 0.152 g, 1.168 mmol), and DPP (0.292 g, 1.168 mmol) were added to a Schlenk flask. The resulting solution was purged with N_2 during 30 min. Subsequently, the flask was closed and immediately immersed in an oil bath at 100 °C to start the ROP under continuous stirring. After 24 h, cooling down to room temperature and opening the flask to air stopped the polymerization. The resulting polymer was obtained by precipitation in cold methanol, and dried under vacuum until constant weight.

P(HEMA-*g*-PCL)-*b*-PCL copolymers (samples COP1, COP2, and COP3) were then prepared by RAFT polymerization of mPCL macromonomer using the PCL macroCTA under conventional Schlenk techniques already reported elsewhere.[30] The mPCL macromonomer (0.5 g, 0.25 mmol), PCL macroCTA (0.02 g, 0.0125 mmol), VAZO catalyst 88 (0.0008 g, 0.0031 mmol), and toluene (4.0 mL) were added to the Schlenk flask, and the mixture was purged with N_2 by 30 min. The reaction was started when the flask was immersed in an oil bath at 100 °C under continuous stirring. After a given polymerization time (usually, 24 h), the reaction was stopped by cooling down the flask to room temperature and opening it to air. The final product was obtained by precipitation in cold methanol and vacuum drying. The degree of polymerization of PCL was determined by independent SEC analysis of the mPCL macromonomer and the PCL macroCTA. Then, the degree of polymerization of the mPCL macromonomer after RAFT polymerization was determined as described earlier elsewhere.[33,35]

2.1.2. Synthesis of P(HEMA-*co*-HEMA-*g*-PCL)-*b*-PCL by a Combined "Grafting Through" and "Grafting From" Method Consisting in Simultaneous RAFT and ROP Processes

P(HEMA-*co*-HEMA-*g*-PCL)-*b*-PCL copolymers (samples COP4, COP5, and COP6) were synthesized in a one-pot RAFT and ROP polymerization procedure. In a typical reaction, the RAFT and ROP coinitiator agent BSTSE (12.7 mg, 0.052 mmol), HEMA monomer (0.31 mL, 2.57 mmol), ε-CL monomer (3.0 mL, 26.28 mmol), Vazo-88 radical initiator (3.1 mg, 0.0129 mmol), dry toluene (3.2 mL), and DMF (0.2 mL, as internal reference for NMR spectroscopy conversion analysis) were placed in a dry 100 mL Schlenk flask equipped with a stirrer. The tube was closed, subjected to three freeze–pump–thaw cycles, and subsequently backfilled with nitrogen gas. The ROP catalyst DPP (13.0 mg, 0.052 mmol) was then added under gentle nitrogen flow and the flask was closed and immediately immersed in an oil bath at 100 °C to start the polymerization. The polymerization was stopped after a given time by cooling down to room temperature and opening the flask to air. The final product was obtained after precipitation in cold methanol and vacuum drying.

2.2. Chemical Characterization

2.2.1. Nuclear Magnetic Resonance

^{1}H-NMR spectra were acquired using an Avance DPX 400 spectrometer (400 MHz for H, 100 MHz for C). The spectra were obtained by dissolving a small quantity of the polymer sample (≈ 50 mg), at room temperature, using $CDCl_3$ as solvent.

2.2.2. Fourier Transform Infrared Spectroscopy

FTIR spectra of copolymers were obtained on a Nicolet FTIR 520 spectrometer. Cast films from copolymer solutions (1 wt% in chloroform) were obtained onto NaCl windows. FTIR spectra were recorded at 4 cm^{-1} resolution over the 4000–400 cm^{-1} range, using an accumulation of 40 scans and air as the background.

2.2.3. Size Exclusion Chromatography

Polymer samples were characterized by SEC on a system built with a Waters 515 HPLC pump and a Waters model 410 differential refractometer detector, equipped with three mixed bed Phenogel linear (2) columns and a precolumn with 5 mL bead size (Phenomenex). The solvent employed was toluene flowing at a rate of 1 mL min^{-1}. The injection volume was 200 μL, and polystyrene (PS) standards were used for calibration. The Mark–Houwink calibration constants used were $K_{PS} = 0.012$ mL g^{-1}, $\alpha_{PS} = 0.71$ for PS[36] and $K_{PCL} = 0.01298$ mL g^{-1}, $\alpha_{PCL} = 0.828$ for PCL.[37]

2.2.4. Thermogravimetric Analysis

Thermal degradation was carried out in a TA Instrument Discovery Series thermogravimetric balance. Samples were heated from 30 to 700 °C at 10 °C min^{-1}, employing air and nitrogen (25 mL min^{-1}). Curves of weight loss as a function of temperature were recorded and the maximum decomposition temperature of each component was obtained from first derivative curves.

2.2.5. Differential Scanning Calorimetry

DSC analyses were performed on a Pyris 1 Perkin-Elmer equipment. Samples for crystallization experiments were measured under N_2 atmosphere. ≈ 0.01 g of each polymer was employed. All samples were heated from 30 to 90 °C at 10 °C min^{-1} in order to obtain the heat of fusion (ΔH_m) from the second heating.

2.2.6. Nonisothermal Crystallization Tests

As already discussed, the proper understanding of thermal properties of homogeneous branched block copolymers is necessary to predict the behavior of polymer melts, since many commercial polymer commodities are, in fact, composed of branched fractions. Therefore, nonisothermal crystallization experiments were carried out by using the following sequential steps: first, the sample was heated from 30 to 90 °C at 10 °C min^{-1}. Then, it was kept at 90 °C during 5 min and cooled at different rates, ranging from 2 to 10 °C min^{-1}, following a procedure already reported in the literature.[12,38,39]

3. Results and Discussion

The copolymers used in this study were synthesized by two different reaction pathways, which enabled the control over the distribution of branching. Samples prepared by a "grafting through" or macromonomer method produced comb-shaped structures (Scheme 1), since each monomeric unit bears a polymeric chain as a side group. Depending

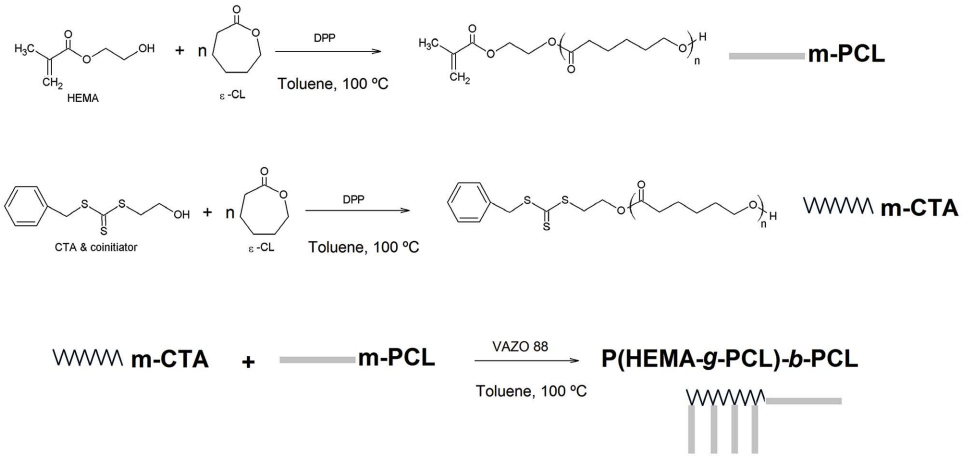

Scheme 1. Synthesis of precursors and P(HEMA-*g*-PCL)-*b*-PCL copolymers.

on the graft density and degree of polymerization, the resulting P(HEMA-*g*-PCL)-*b*-PCL comb-like polymers adopt several conformations.

Other set of samples was prepared by combining the "grafting through" and the "grafting from" methods (Scheme 2). This was achieved in a one-pot RAFT and ROP reaction by the presence of BSTSE that had a dual role: the thiocarbonylsulfanyl moiety functioned as CTA in the RAFT process of HEMA monomer, whereas the hydroxyl group initiated the ROP reaction, with both polymerizations occurring at the same time. Concurrently, the ROP process was initiated by two groups: hydroxyl groups of unreacted HEMA and hydroxyl groups of the BSTSE. Therefore, the RAFT reaction progressively incorporates HEMA monomer and HEMA-PCL macromonomer, thus leading to a less dense packing of branches.

3.1. Physicochemical Characterization

Macromolecular characteristics of P(HEMA-*g*-PCL)-*b*-PCL and P(HEMA-*co*-HEMA-*g*-PCL)-*b*-PCL samples used in this study are given in Table 1. In all cases, the polymers showed narrow molar mass distributions with polydispersity values (M_w/M_n) lower than 1.2, as calculated from the SEC chromatograms, hence indicating good control over the block copolymerization (nevertheless COP2 has an M_w/M_n a little bit higher compared to the other copolymers. This fact might be explained by uncompleted removal of air during the purging process). M_n values obtained by SEC are clearly offset due to the use of PS standards with distinct hydrodynamic volume from that of the samples. M_n was not determined by NMR because the resonance of protons from the CTA fragment (as well as from end-groups) became almost undetectable for the long polymer chains due to reasons discussed in the literature.[40] Therefore, we reported macromolecular dimensions corresponding to the theoretical molar mass, M_n, which was calculated from conversion data obtained from ^{1}H NMR analysis of aliquots taken from the reaction and diluted with $CDCl_3$ assuming quantitative reaction of the CTA, and purified polymer samples (after precipitation). The high efficiency (near quantitative reaction) of the CTA in initiating the ROP process and in mediating the RAFT polymerization has been previously verified by our group.[30]

Figure 1 shows a representative ^{1}H-NMR spectrum of P(HEMA-*co*-HEMA-*g*-PCL)-*b*-PCL (COP4) copolymer before purification by successive precipitation in methanol. The ^{1}H-NMR spectrum was interpreted in light of the comprehensive peak assignments based on 2D ^{1}H–^{1}H and ^{1}H–^{13}C NMR studies reported by Le Hellaye et al.[41] The inset of Figure 1 shows characteristic peaks of methacrylic backbones, indicating the successful growth of the PHEMA chain in the copolymer despite the well-known weakness of this signal in $CDCl_3$.[2,3,40] The two pendent methylene groups of the HEMA units directly linked to the PCL-grafted chains (signals *e* and *f*, or *e′* and *f′*) are clearly identified in the spectrum and proved the initiation of ε-CL monomer by HEMA monomer units. Since the sample also contains the unreacted HEMA-PCL macromonomer, this species appears in the spectrum together with the copolymer. The ratio of unreacted HEMA-PCL was determined from signals *l*, *d* and *a′*. HEMA conversion (*Y* values shown in the chemical structure inset in Figure 1) was determined using DMF as an internal reference. The degree of polymerization of PCL (*n* values in Figure 1) was calculated from the integral ratio between PCL main chain

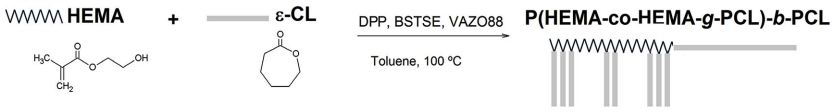

Scheme 2. Synthesis of P(HEMA-*co*-HEMA-*g*-PCL)-*b*-PCL copolymers.

Table 1. Chemical and thermal characterizations of PCL and PCL-based copolymers synthesized.

Polymer[a)]	Name	M_n[c)] [g mol^{-1}]	M_w/M_n[c)]	T_m[d)] [°C]	X_c[d)] [%]	T_{max}[e)*] [°C]	T_{max}[e)#] [°C]
Linear poly(ε-caprolactone)	PCL[b)]	11 000	1.14	56.9	44.7	405.2	407.1
P(HEMA$_{10}$-*g*-PCL$_3$)-*b*-PCL$_7$	COP1	5500	1.10	53.6	33.4	403.4	401.9
P(HEMA$_8$-*g*-PCL$_5$)-*b*-PCL$_{15}$	COP2	7300	1.30	50.5	35.2	404.6	406.5
P(HEMA$_{12}$-*g*-PCL$_5$)-*b*-PCL$_{15}$	COP3	9900	1.16	50.1	35.8	410.1	413.1
P(HEMA$_{10}$-*co*-HEMA$_{35}$-*g*-PCL$_7$)-*b*-PCL$_7$	COP4	32 300	1.19	41.1	34.9	407.6	398.6
P(HEMA$_7$-*co*-HEMA$_{38}$-*g*-PCL$_8$)-*b*-PCL$_8$	COP5	38 600	1.13	38.2	32.2	409.3	390.2
P(HEMA$_3$-*co*-HEMA$_{27}$-*g*-PCL$_{14}$)-*b*-PCL$_{14}$	COP6	46 000	1.11	42.9	33.7	407.9	387.9

[a)]Number of branches of PCL and HEMA for each copolymer determined by (^{1}H-NMR analysis); [b)]*Model* PCL homopolymer obtained by anionic polymerization[32]; [c)]Number-average molar mass (M_n) and polydispersity (M_w/M_n) determined by SEC; [d)]Melting temperature (T_m) and percentage of crystallinity (%X_c) determine by DSC, using $\Delta H_{100\%}$ = 136.1 J g^{-1} for 100% crystalline poly(ε-caprolactone)[48]; [e)]Temperature at maximum degradation rate (T_{max}) under N_2(•) and oxidative atmosphere (#), respectively.

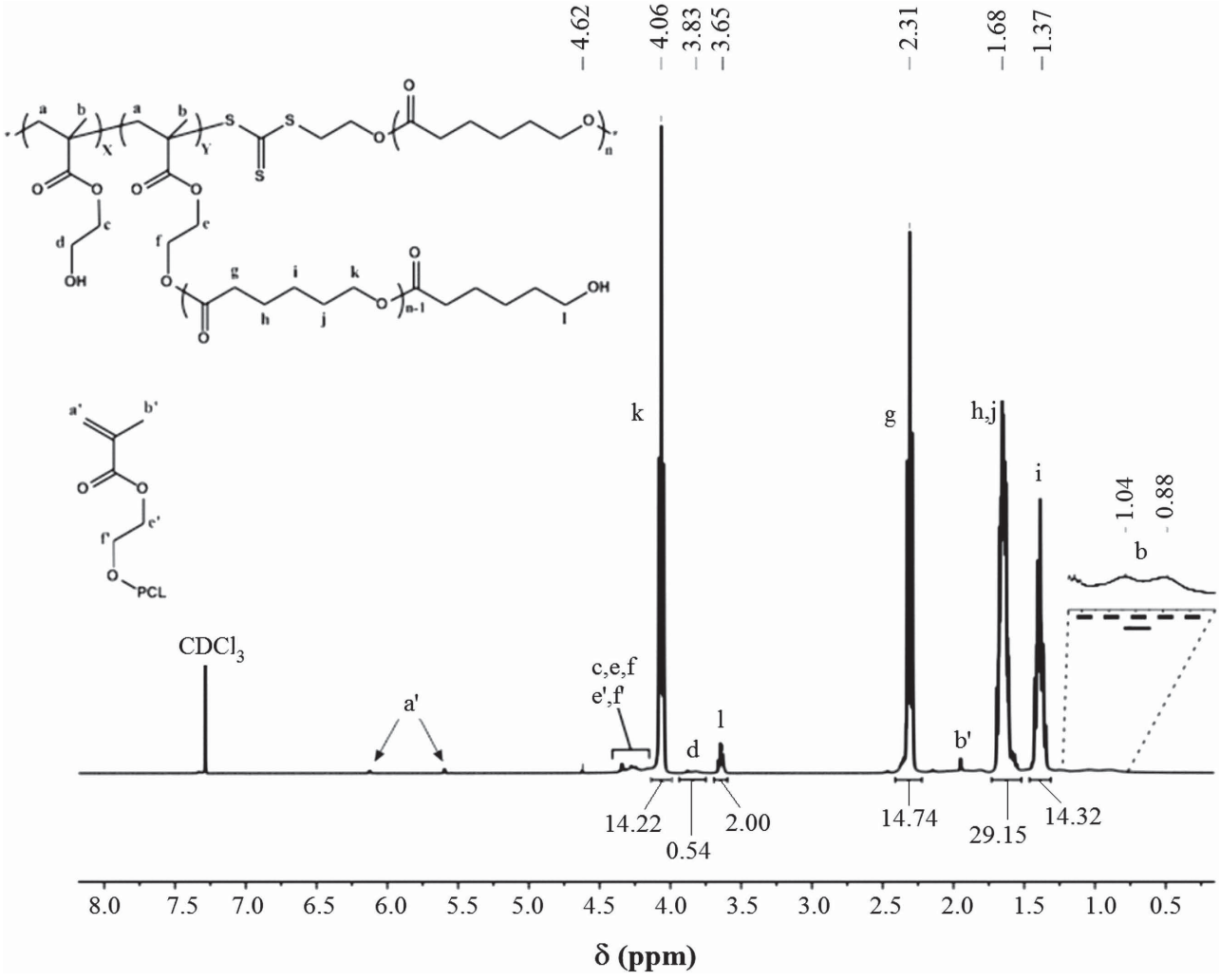

Figure 1. ^{1}H-NMR spectrum of P(HEMA-*co*-HEMA-*g*-PCL)-*b*-PCL, copolymer (COP4).

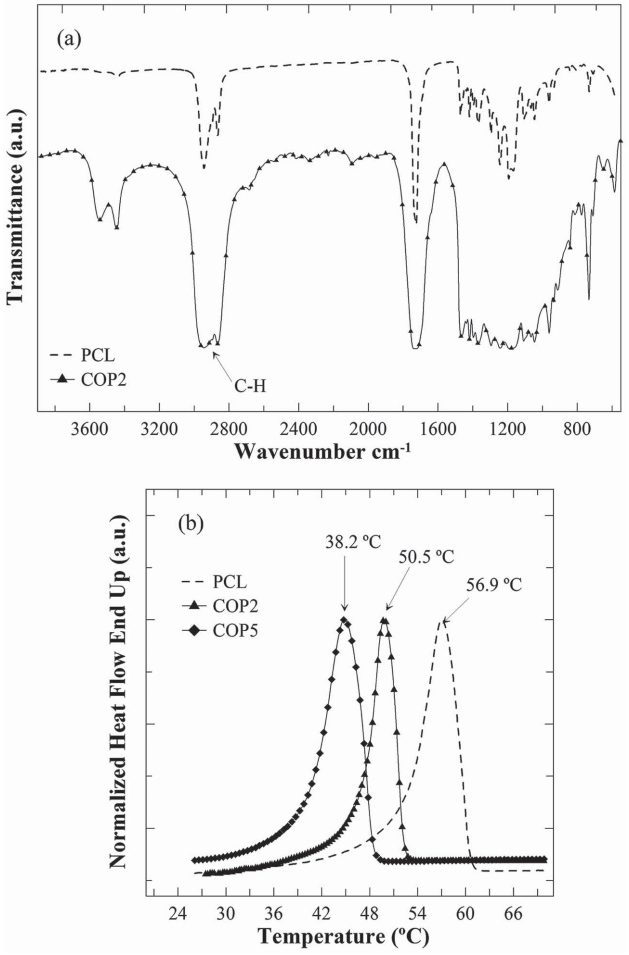

Figure 2. a) FTIR spectra of PCL and P(HEMA-*g*-PCL)-*b*-PCL (COP2) copolymer. b) DSC curves of PCL, P(HEMA-*g*-PCL)-*b*-PCL (COP2), and P(HEMA-*co*-HEMA-*g*-PCL)-*b*-PCL (COP5).

signal (C(O)C***H***$_2$CH$_2$..., 2n H) at δ = 2.31 ppm (peak denoted as *g*) relative to the methylene end-group of the same chain (PCL-C***H***$_2$OH, 2H) at δ = 3.65 ppm (peak denoted as *l*).

The purification of samples containing unreacted HEMA-PCL macromonomer can be achieved by successive precipitation in methanol from toluene, as formerly reported by Le Hellaye et al.[41] The removal of free HEMA-PCL can be confirmed by SEC analysis (Figure S1, Supporting Information).

FTIR spectra shown in Figure 2a display the characteristic absorption band for PCL at 2960 and 2865 cm^{-1} (ν_{CH}). A strong and narrow band due to the stretching vibration of carbonyl groups ($\nu_{C=O}$) appears at 1724 cm^{-1}. Bands corresponding to the O–C=O bonds are evident at 1260 and 1191 cm^{-1}, whereas a small band assigned to $(-CH_2)_n$ with $n > 4$ can be seen at 732 cm^{-1}.[28,32] Block copolymers (COP 2) show a more intense signal at 2920 and 2850 cm^{-1} due to C–H bond from methylene groups. In addition, the copolymer spectra feature typical vibrational bands corresponding to the C=O group of PHEMA and PCL segment (1728, 1240, and 1174 cm^{-1}), and C=S bond from the CTA end group (1066 cm^{-1}).[22,41]

3.2. Thermal Characterization

DSC analysis showed a noticeable reduction in the melt point temperature for all comb-like copolymers. As an example, Figure 2b compares linear PCL and the copolymers obtained by the two methodologies employed. Thermal analysis showed a decrease of the melting point (T_m) and the degree of crystallinity (X%) with the presence of branches. In the particular case of T_m, a reduction of ≈ 20 °C was detected, as well as a reduction of ≈ 28% in X%. These results are a clear indication that the presence of branches in the block copolymers affect the crystallization process.[12] The results obtained in our work agree well with those observed by Choi & Kwak for hyperbranched PCL (HPCL).[2] According to this work, the T_m values of HPCLs are all lower than that of LPCL and gradually decreased as the degree of branching became increased, which is expected because the presence of branches in a branched polymer may render crystallization more difficult than in a linear polymer. In the case of the comb-like copolymers of this work, those copolymers with higher branching density (COP4, COP5, and COP6) show the lower T_m values. Another fact that can be observed in Table 1 is the effect of the polymerization degree (DP) of the PCL branches. It seems that, as in the case of the branching degree, when the length of the branches increases, the T_m values decrease. This effect can be easily shown in Figure 2b in which the DSC curves of LPCL COP2 and COP5 are displayed for comparative purposes.

Thermogravimetric measurements were used to evaluate the degradation processes of *model* PCL and the obtained copolymers as a function of temperature. Figures 3 and 4 show the TGA and first-derivative curves under nitrogen and oxygen atmospheres, respectively. *Model* PCL showed one thermal event at around 405–410 °C, as it is reported in the literature.[32,42,43] As it can be observed, PHEMA incorporation did not affect the maximum degradation rate (T_{max}) of the linear polyester (Figure 3b and Table 1), but a decrease in the initial zone between 180 and 350 °C was observed. This reduction on the thermal stability of all copolymers, under nitrogen atmosphere, could be attributed to the presence of PHEMA.[43,44]

TGA measurements under oxidative atmosphere show two weight loss steps. The first one corresponds to PCL decomposition at around 410 °C, and the final event (≈ 550 °C) is well known as "glowing combustion" process (Figure 4a). In the case of the copolymers, due to the presence of PHEMA, the degradation proceeds in three steps, at ≈ 250, ≈ 380, and ≈ 500 °C, respectively. The first step corresponds to the typical degradation of PHEMA as it

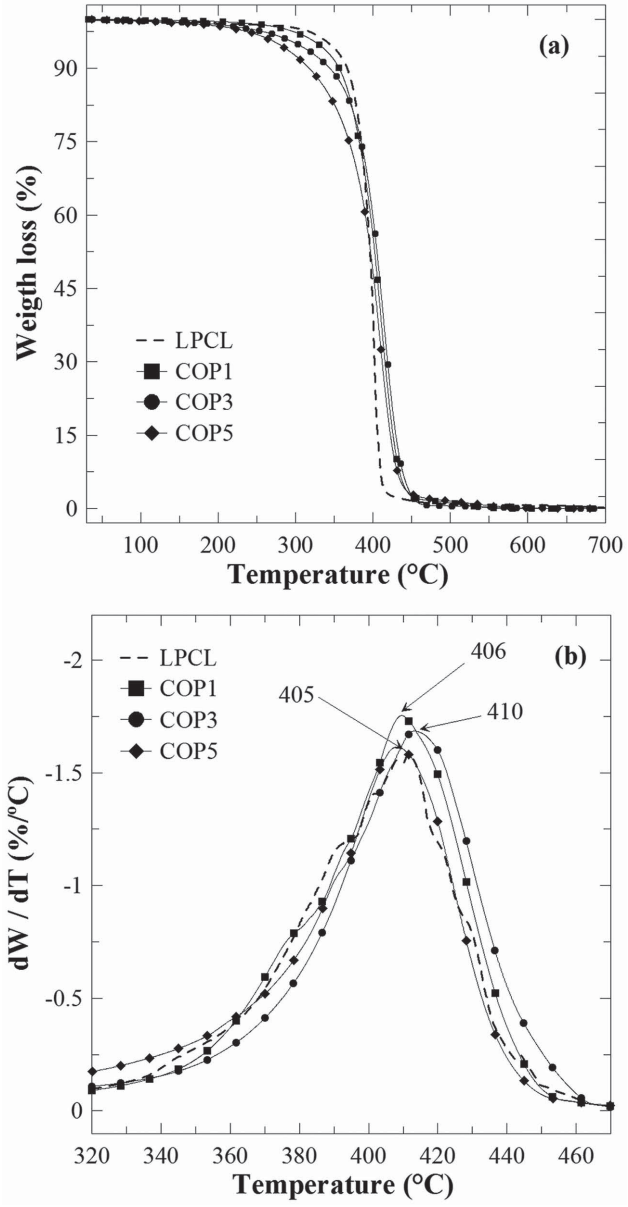

Figure 3. a) TGA curves, under nitrogen atmosphere, of PCL, P(HEMA-*g*-PCL)-*b*-PCL (COP1, COP3), and P(HEMA-*co*-HEMA-*g*-PCL)-*b*-PCL (COP5); b) first-derivative TGA curves.

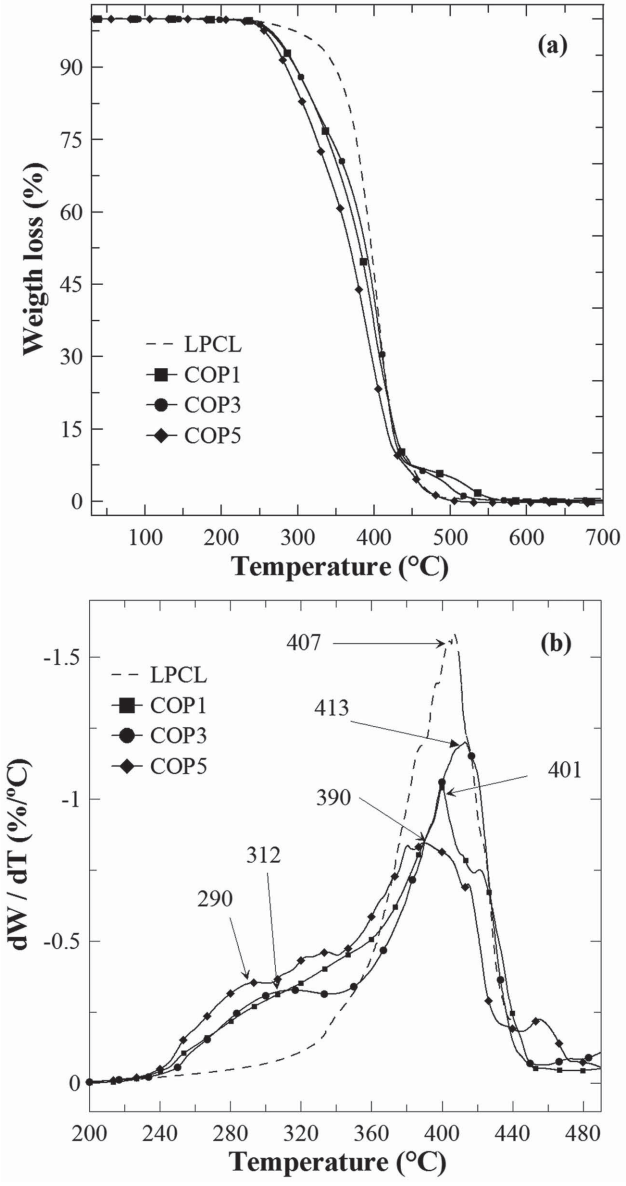

Figure 4. a) TGA curves, under oxygen atmosphere, of PCL, P(HEMA-*g*-PCL)-*b*-PCL (COP1, COP3), and P(HEMA-*co*-HEMA-*g*-PCL)-*b*-PCL (COP5); b) first-derivative TGA curves.

was reported in the literature,[32,43,44] the second step at lower values corresponds to PLC degradation, and the last step is associated with the glowing combustion process. As it can be clearly observed, the presence of PHEMA produces, under oxidative conditions, a slight decrease (≈10 °C) in the T_{max} of the PCL, compared to *model* PCL (Figure 4b).

3.3. Kinetic Measurements

Figure 5 shows representative DSC curves of heat flow as a function of temperature at different cooling rates for the linear polyester (a) and COP 5 copolymer (b), respectively. Essentially the same profile is observed for other copolymer samples.

The values of crystallization temperature (T_c) and the half-life time ($t_{1/2}$) for *model* PCL and all copolymers studied are summarized in Table 2. Crystallization temperatures (T_c) correspond to the exothermic peak maxima, and $t_{1/2}$ is the necessary time for 50% of the total crystallization to occur.

It can be noticed that $t_{1/2}$ decreases gradually at higher cooling rate for all materials; however, highest $t_{1/2}$ values were observed in the case of the copolymers obtained by the simultaneous ROP and RAFT polymerization,

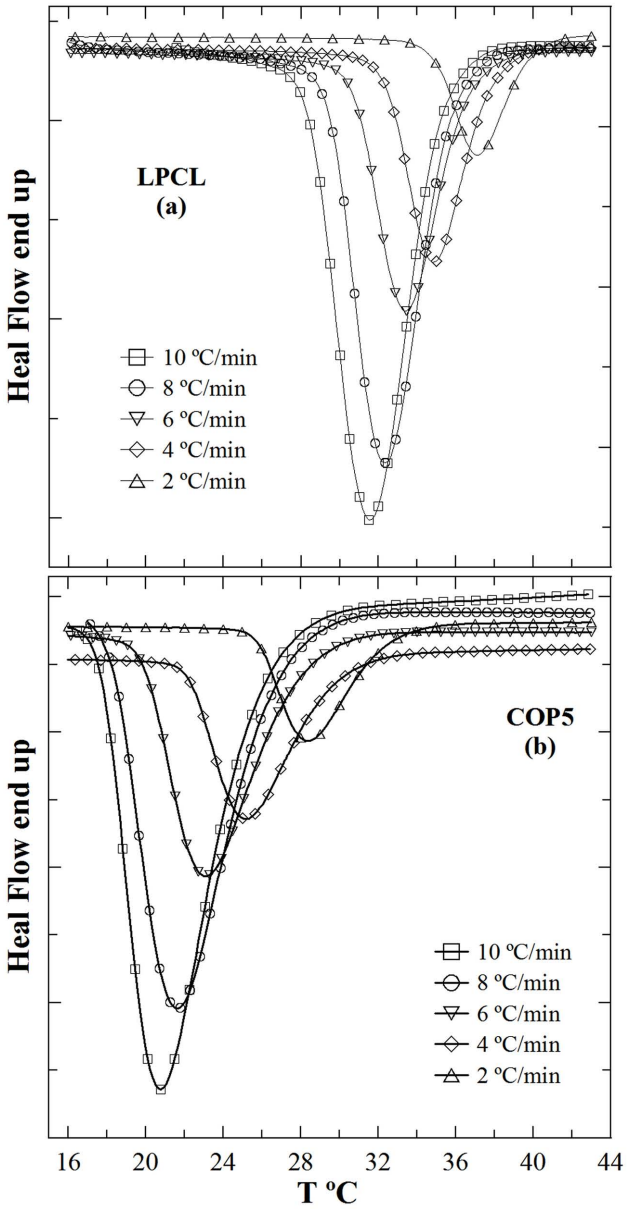

Figure 5. DSC endothermic curves for nonisothermal crystallization of a) linear PCL and b) P(HEMA-*co*-HEMA-*g*-PCL)-*b*-PCL (COP5).

$t_{1/2\ COP4\text{-}COP6} >> t_{1/2\ PCL}$ (Figure 6). In contrast, lower $t_{1/2}$ was detected for COP1 and COP2 than *model* PCL (Figure 6). Probably, the behavior observed for COP1 and COP2 could be attributed to the closeness and the short-length branches that induce a faster crystallization.[2,12]

Crystallization behavior was followed using DSC analysis to obtain the relative crystallinity, X_T, as a function of temperature (T) by using Equation (1)[36]

$$X_T = \frac{\int_{T_0}^{T_\infty} (dH_c/dT)dT}{\int_{T_0}^{T} (dH_c/dT)dT} \quad (1)$$

Table 2. Crystallization peak temperature, T_c, half-time, $t_{1/2}$, and activation energy of crystallization for PCL and PCL-based copolymers.

Sample	Crystallization parameter	Cooling rate (°C min^{-1})				
		2	4	6	8	10
PCL	T_c (°C)	31.5	32.3	33.6	34.8	37.1
	$t_{1/2}$ (min)	26.5	13.1	9.5	7.3	5.9
COP1	T_c (°C)	31.9	32.0	33.0	34.9	36.7
	$t_{1/2}$ (min)	18.6	9.8	6.9	5.2	4.3
COP2	T_c (°C)	32.6	30.1	28.5	28.3	28.1
	$t_{1/2}$ (min)	18.6	9.9	7.1	5.4	4.4
COP3	T_c (°C)	38.9	36.7	35.3	34.4	33.7
	$t_{1/2}$ (min)	20.5	10.8	7.7	5.8	4.7
COP4	T_c (°C)	20.8	21.6	23.1	25.2	28.3
	$t_{1/2}$ (min)	30.7	16.2	11.2	8.6	7.1
COP5	T_c (°C)	11.5	11.8	12.4	13.9	14.7
	$t_{1/2}$ (min)	37.5	19.5	13.4	10.3	8.6
COP6	T_c (°C)	10.9	11.5	12.1	13.3	14.2
	$t_{1/2}$ (min)	39.7	21.6	14.3	11.2	9.1

where T_0 and T_∞ are the initial and final crystallization temperatures. Based on this equation, X_T at a specific temperature can be calculated, and the corresponding X_T versus T plots for PCL and two copolymers (COP3 and COP5) are shown in Figure 7. The relationship between crystallization

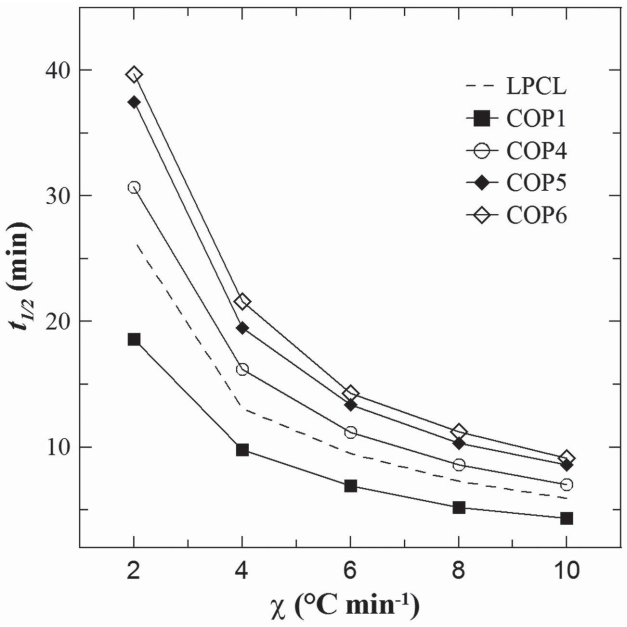

Figure 6. Crystallization half-time $t_{1/2}$ for PCL, P(HEMA-*g*-PCL)-*b*-PCL (COP1), and P(HEMA-*co*-HEMA-*g*-PCL)-*b*-PCL (COP4, COP5, COP6).

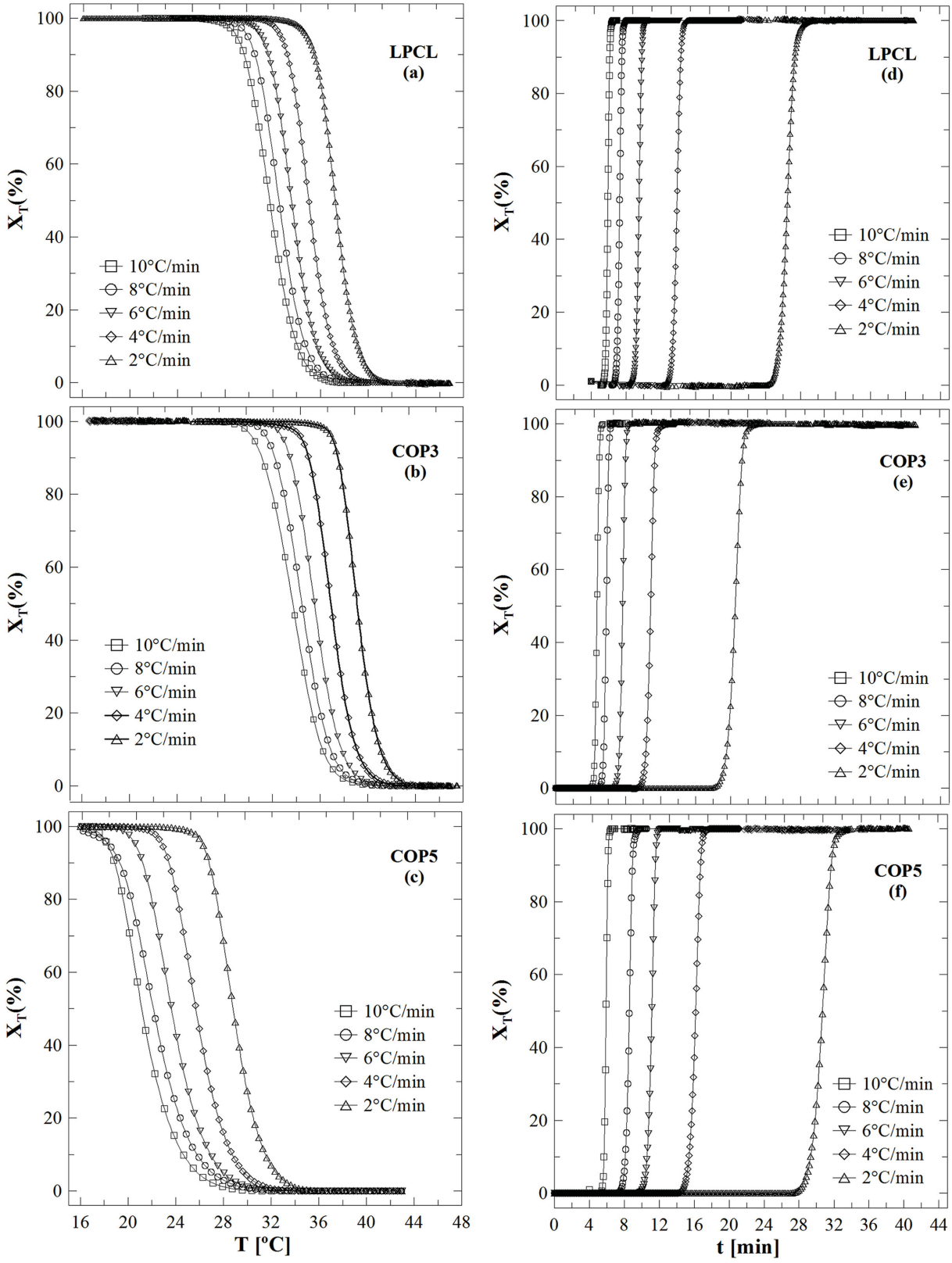

Figure 7. a–c) Crystallinity percentage, X_T (%) versus temperature (T), and d–f) X_T (%) versus time (t), for PCL, P(HEMA-*g*-PCL)-*b*-PCL (COP3), and P(HEMA-*co*-HEMA-*g*-PCL)-*b*-PCL (COP5).

peak temperature and crystallization time (t) during nonisothermal crystallization can be described as follows

$$t = \frac{T_o - T}{\chi} \quad (2)$$

where χ is the cooling rate and T is the same temperature used to determine X_T. According to Equation (1), the relative degree of crystallinity (X_t) can be defined as a function of time (t)

$$X_t = \frac{\int_{t_o}^{t} (dH_c/dt)dt}{\int_{t_o}^{t_\infty} (dH_c/dt)dt} \quad (3)$$

where t_0, and t_∞ are the onset and final crystallization times, respectively, and t is the time used to determine X_t. It can be seen that it takes less time for crystallization to complete at higher cooling rates (Figure 7). In addition, all X_t versus t curves have approximately the same S-shape, indicating that curves tend to become flat at the later stage due to spherulitic impingement.[2,12]

Nonisothermal crystallization kinetics was further analyzed using the Ozawa's model equation, which is an extension from the Avrami's equation originally applied in the isothermal crystallization.[45] Thus, it is assumed that sample is cooled at a constant cooling rate.[30,31] In this case, Equation (4) is applied

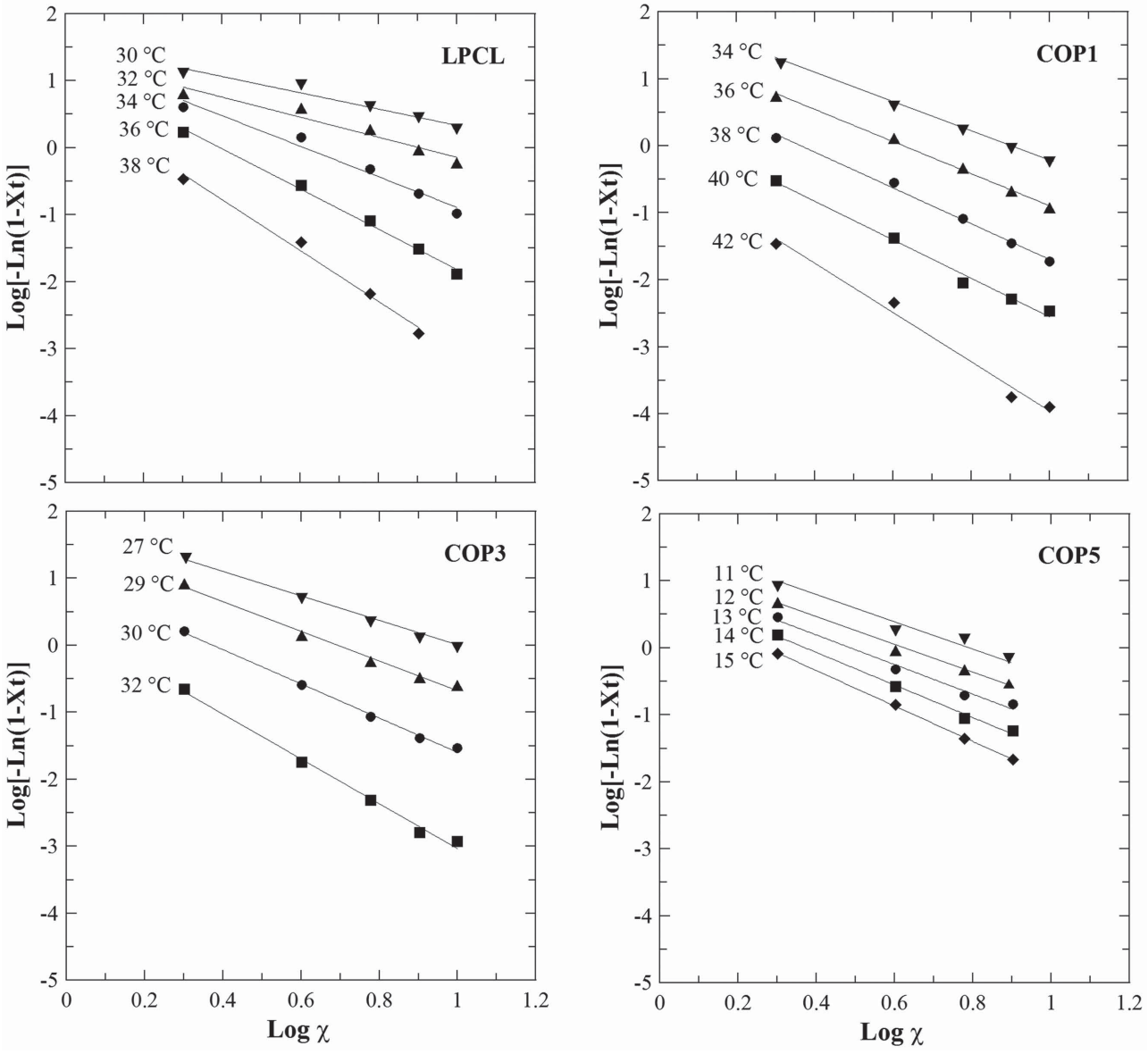

Figure 8. Ozawa plots of log [–ln (1 –X_t)] versus log χ for PCL, P(HEMA-*g*-PCL)-*b*-PCL (COP1, COP3), and P(HEMA-*co*-HEMA-*g*-PCL)-*b*-PCL (COP5) at various cooling rates. Symbols correspond to experimental points, and solid lines corresponds to the fitting of Equation (5).

Table 3. Ozawa exponent, *m*, and cooling function, *K*(*T*), for PCL and PCL-based copolymers.

T [°C]	PCL		COP1		COP2		COP3		COP4		COP5		COP6	
	m	log *K*(*T*)	*m*	log *K*(*T*)	*m*	log *K*(*T*)	*m*	log *K*(*T*)	*m*	log *K*(*T*)	*m*	log *K*(*T*)	*m*	log *K*(*T*)
42	–	–	3.7	0.2	–	–	–	–	–	–	–	–	–	–
40	–	–	2.9	0.3	–	–	–	–	–	–	–	–	–	–
38	3.8	0.7	2.7	0.9	2.9	0.7	–	–	–	–	–	–	–	–
36	2.9	1.1	2.4	1.5	2.1	1.1	–	–	–	–	–	–	–	–
34	2.3	1.3	2.1	1.8	1.6	1.2	–	–	–	–	–	–	–	–
32	1.5	1.4	–	–	1.1	1.3	3.3	0.3	–	–	–	–	–	–
30	1.2	1.5	–	–	1.2	1.7	2.5	0,9	–	–	–	–	–	–
29	–	–	–	–	–	–	2.2	1.5	2.9	0.7	–	–	–	–
27	–	–	–	–	–	–	1.8	1.8	2.7	1.1	–	–	–	–
25	–	–	–	–	–	–	3.3	2.3	2.5	1.4	–	–	–	–
23	–	–	–	–	–	–	–	–	2.1	1.5	–	–	–	–
21	–	–	–	–	–	–	–	–	1.8	1.7	–	–	–	–
15	–	–	–	–	–	–	–	–	–	–	2.6	0.7	2.5	0.7
14	–	–	–	–	–	–	–	–	–	–	2.4	0.9	2.4	0.8
13	–	–	–	–	–	–	–	–	–	–	2.2	1.1	2.2	0,9
12	–	–	–	–	–	–	–	–	–	–	2.1	1.3	2.1	1.1
11	–	–	–	–	–	–	–	–	–	–	1.8	1.4	1.9	1.2

$$X_t = 1 - \exp\left[\frac{-K(T)}{\chi^m}\right] \quad (4)$$

where *K*(*T*) is the Ozawa's crystallization cooling function and *m* is the Ozawa's exponent, which depends on the dimension of crystal growth. Applying double logarithm to both sides of Equation (4), Equation (5) is obtained

$$\log[-\ln(1 - X_t)] = \log K(T) - m \log \chi \quad (5)$$

The results obtained show that Ozawa's equation described successfully the nonisothermal crystallization process, presenting a good linearity between experimental and theoretical values. Figure 8 shows Ozawa's plots of log [ln (1 – X_t)] versus log χ for the linear PCL and the three copolymers studied (COP1, COP3, and COP5). The remaining results are summarized in Table 3. Ozawa's exponent, *m*, and the cooling function, *K*(*T*), for all copolymers were estimated from the slope and the intercept of the plots, respectively (Table 3). Ozawa's exponent values show little changes for the different samples, whereas the cooling functions are shown to be much influenced by the specific architecture of the different copolymers.[12]

Figure 9 shows the cooling functions *K*(*T*) versus *T* for *model* PCL and some copolymers. Results show that *K*(*T*) increase at lower crystallization temperature. This effect could be attributed to polymeric flow features, since viscosity increases at lower temperatures which makes difficult the transport of polymer chains to the growth front. Considering that the cooling function is a function of

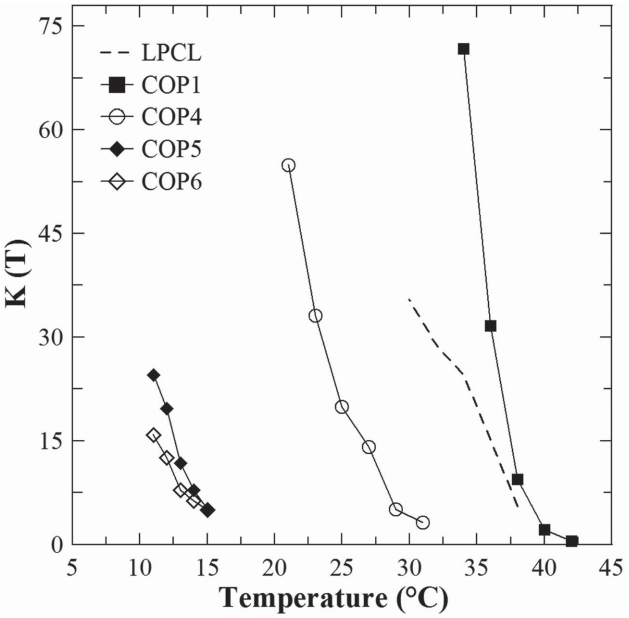

Figure 9. Cooling functions *K*(*T*) for PCL, P(HEMA-*g*-PCL)-*b*-PCL (COP1), and P(HEMA-*co*-HEMA-*g*-PCL)-*b*-PCL (COP4, COP5, COP6) at various temperatures.

nucleation and growth rate, the results of $K(T)$ indicate that crystallization is retarded for the branched copolymers. Values of $K(T)$ for all copolymers are also lower than that for PCL (with the exception of COP1 and COP2) at a specific temperature, which indicates that nucleation and growth rate for grafted copolymers are lower than for *model* PCL. This observation is in good agreement with $t_{1/2}$ results.

4. Conclusions

Branched copolymers were obtained by ROP and RAFT polymerization using ε-CL and HEMA, employing two different synthesis methodologies. Obtained copolymers displayed controlled molar masses and low M_w/M_n values. NMR, FTIR, and SEC analyses confirm the presence of PHEMA and PCL in the materials and are a clear evidence of the synthesis of the targeted copolymers. Nonisothermal crystallization of branched copolymers was studied and compared with the corresponding *model* PCL. Thermal analysis indicates that the presence of branches reduced the melting-point temperature without compromising their thermal stability. In general, a decrease in the crystallization rate was obtained by increasing the number of branches in the copolymers. These phenomena are ascribed to the polymer architecture, which is noticeably affected by the absence or the presence of branches in the main chain. This observation agrees well with crystallization time values that gradually decrease, at a specific cooling rate, with an increase in the number of branches in the copolymers. Crystallization kinetics was analyzed by Ozawa's method and obtained results satisfactorily describe the nonisothermal crystallization behavior.

Supporting Information

Supporting Information is available from the Wiley Online Library or from the author.

Received: July 6, 2015; Revised: September 3, 2015; Published online: November 17, 2015; DOI: 10.1002/macp.201500248

Keywords: branched copolymers; poly(2-hydroxyethylmethacrylate) (PHEMA); poly(ε-caprolactone) (PCL); RAFT and ROP polymerization; thermal behavior

[1] D. Uhrig, J. Mays, *Polym. Chem.* **2011**, *2*, 69.
[2] J. Choi, S. Kwak, *Macromolecules* **2003**, *36*, 8630.
[3] W. Yuan, J. Yuan, F. Zhang, X. Xie, C. Pan, *Macromolecules* **2007**, *40*, 9094.
[4] D. Lanson, F. Ariura, M. Schappacher, R. Borsali, A. Deffieux, *Macromolecules* **2009**, *42*, 3942.
[5] S. Christodoulou, H. Iatrou, D. Lohse, N. Hadjichristidis, *J. Polym. Sci., Part A: Polym. Chem.* **2005**, *43*, 4030.
[6] A. Shinozaki, D. Jasnow, A. Balazs, *Macromolecules* **1994**, *27*, 2496.
[7] V. Palyulin, I. Potemkin, *Polym. Sci., Ser. A* **2007**, *49*, 473.
[8] M. Runge, S. Dutta, N. Bowden, *Macromolecules* **2006**, *39*, 498.
[9] H. Chen, J. Jia, W. Zhang, J. Kong, *Polym. Test.* **2014**, *35*, 28.
[10] J. Jang, J. Oh, *Polymer* **1999**, *40*, 5985.
[11] J. Zhang, C. Hu, *Eur. Polym. J.* **2008**, *44*, 3708.
[12] J. Choi, S. Chun, S. Kwak, *Macromol. Chem. Phys.* **2006**, *207*, 1166.
[13] L. Atanase, O. Glaied, G. Riess, *Polymer* **2011**, *52*, 3074.
[14] G. Eastmond, *Adv. Polym. Sci.* **2000**, *149*, 61.
[15] M. Woodruff, D. Hutmacher, *Prog. Polym. Sci.* **2010**, *35*, 1217.
[16] L. Ludueña, V. Alvarez, A. Vazquez, *Mater. Sci. Eng. A* **2007**, *121*, 460.
[17] L. Ludueña, *LN. III Enc. Jov. Inv. Ciencia y Tecnol. Mat.*, Book of Abstracs (electronic format), **2010**, 1.
[18] S. Atzet, S. Curtin, P. Trinh, S. Bryant, B. Ratner, *Biomacromolecules* **2008**, *9*, 3370.
[19] J. Heuschen, J. Vion, R. Jerome, P. Teyssii, *Macromolecules* **1989**, *2451*, 2446.
[20] V. Balsamo, F. Von Gylden, R. Stadler, *Macromol. Chem. Phys.* **1996**, *197*, 1159.
[21] A. Lorenzo, M. Arnal, J. Albuerne, A. Müller, *Polym. Test.* **2007**, *26*, 222.
[22] T. Xu, J. Zhu, C. Yuan, Q. Yang, K. Cui, C. Li, *Eur. Polym. J.* **2014**, *54*, 109.
[23] X. Song, W. Yao, G. Lu, Y. Li, X. Huang, *Polym. Chem.* **2013**, *4*, 2864.
[24] L. Bostan, S. A. Trunfio-Sfarghiu, L. Verestiuc, M. Popa, F. Munteanu, J. Rieu, *Tribol. Int.* **2012**, *46*, 215.
[25] D. Gregonis, G. Russell, J. Andrade, A. DeVisser, *Polymer* **1978**, *19*, 1279.
[26] J. Oh, K. Matyjaszewski, *J. Polym. Sci., Part A: Polym. Chem.* **2006**, *44*, 3787.
[27] A. Hirao, H. Kato, K. Yamaguchi, S. Nakahama, *Macromolecules* **1986**, *24*, 1294.
[28] B. Garipcan, N. Bereli, S. Patır, Y. Arıca, A. Denizli, *Macromol. Biosci.* **2001**, *1*, 332.
[29] J. Skey, R. O'Reilly, *Chem. Commun.* **2008**, *46*, 4183.
[30] A. De Freitas, S. Trindade, P. Muraro, V. Schmidt, A. Satti, M. Villar, A. Ciolino, C. Giacomelli, *Macromol. Chem. Phys.* **2013**, *214*, 2336.
[31] J. Skey, R. Reilly, *J. Polym. Sci., Part A: Polym. Chem.* **2008**, *46*, 3690.
[32] M. Ninago, A. Satti, A. Ciolino, M. Villar, *J. Therm. Anal. Calorim.* **2013**, *112*, 1277.
[33] M. Arnal, V. Balsamo, F. López-Carrasquero, J. Contreras, M. Carrillo, H. Schmalz, V. Abetz, E. Laredo, A. J. Muller, *Macromolecules* **2001**, *34*, 7973.
[34] V. Balsamo, G. Gil, C. Urbina de Navarro, I. W. Hamley, F. Von Gyldenfeldt, V. Abetz, E. Cañizales, *Macromolecules.* **2003**, *36*, 4515.
[35] F. D'Agosto, M. Charreyre, L. Veron, M. Llauro, C. Pichot, *Macromol. Chem. Phys.* **2001**, *202*, 1689.
[36] J. E. Mark, *Polymer Data Handbook*, Oxford University Press, Oxford **1999**.
[37] H. Sun, L. Mei, C. Song, X. Cui, P. Wang, *Biomaterials* **2006**, *27*, 1735.
[38] S. S. Ray, in *Clay-containing Polymer Nanocomposites: From Fundamentals to Real Applications*, (Ed: Suprakas Sinha Ray) Elsevier, Amsterdam **2013**, Ch. 9.

[39] W. Yam, J. Ismail, H. Kammer, M. Lechner, C. Kummerlöwe, *Polymer* **2000**, *41*, 9073.
[40] H. Friebolin, *Basic One- and Two-Dimensional NMR Spectroscopy*, Wiley-VCH, New York **2011**.
[41] M. Le Hellaye, C. Lefay, T. Davis, M. Stenzel, *J. Polym. Sci., Part A: Polym. Chem.* **2008**, *46*, 3058.
[42] S. Murphy, G. Leeke, M. Jenkins, *J. Therm. Anal. Calorim.* **2011**, *107*, 669.
[43] J. Cai, Z. Xionga, M. Zhou, J. Tan, F. Zeng, M. Ma, S. Lin, H. Xiong, *Carbohydr. Polym.* **2014**, *102*, 746.
[44] J. Peterson, S. Vyazovkin, C. Wight, *Macromol. Rapid Commun.* **1999**, *20*, 480.
[45] A. Figueiredo, A. Figueiredo, A. Aonso-Varona, S. Fernandes, T. Palomares, E. Rubio-Azpeitia, A. Barros-Timmons, A Silvestre, C. Pascoal, C. Freire, *BioMed Res. Int.* **2013**, *2013*, 1.
[46] T. Ozawa, *Polymer* **1971**, *12*, 150.
[47] A. Jeziorny, *Polymer* **1978**, *19*, 1142.
[48] W. Yam, J. Ismail, H. Kammer, H. Schmidt, C. Kummerlöwe, *Polymer* **1999**, *40*, 5545.